

We are IntechOpen, the world's leading publisher of Open Access books Built by scientists, for scientists

6,900

Open access books available

185,000

International authors and editors

200M

Downloads

Our authors are among the

154

Countries delivered to

TOP 1%

most cited scientists

12.2%

Contributors from top 500 universities



WEB OF SCIENCE™

Selection of our books indexed in the Book Citation Index
in Web of Science™ Core Collection (BKCI)

Interested in publishing with us?
Contact book.department@intechopen.com

Numbers displayed above are based on latest data collected.
For more information visit www.intechopen.com



Adsorbed Natural Gas Storage for Vehicular Applications

*Akhoury Sudhir Kumar Sinha, Umaprasana Ojha,
Marriyappan Sivagnanam Balathanigaimani and Sanjay Kar*

Abstract

The use of adsorbed natural gas (ANG) as a transportation fuel is a relatively cleaner alternative compared to that of gasoline and is important from the perspective of environmental safety. However, unlike gasoline and diesel, natural gas requires compression, liquefaction, and adsorption techniques for its storage, as it has a very low volumetric energy density. Among all storage techniques, adsorption-based natural gas (ANG) storage is considered as more economical and relatively safe technology due to its mild temperature and pressure conditions for the storage. This chapter will summarize the recent advances in the area of ANG with reference to various synthetic storage materials recently developed for the purpose and their efficiency towards storage and deliverability of natural gas. Particular emphasis will be given to adsorbents based on porous carbon materials, metal organic frameworks, and covalent organic frameworks for the said application. The synthetic procedure for the above adsorbents, followed by their efficiency to store and deliver natural gas, will be discussed. Finally, in the conclusion, the future scope of the technology will be summarized.

Keywords: adsorbed natural gas storage, metal organic framework, covalent organic framework, vehicular application, porous carbon materials

1. Introduction

The well-known alternative fuels for crude oil-based liquid products are natural gas and hydrogen. Nevertheless, these gaseous fuels require a special storage technique for effective utilization due to their lower volumetric energy density values. Natural gas with wide availability and improved production technology is considered to be an important energy source for the future and a cleaner form of energy compared to that of the higher hydrocarbon-based fuels such as gasoline and diesel due to its low C/H ratio. This consists of mainly methane (55–98 vol%) as the primary component along with other gases such as ethane (2–4 vol%), propane (0.5–2 vol%), and butane (0.25–0.5 vol%) in minor amounts along with few acid gases in trace amounts [1]. An estimate has shown that natural gas produces 55.9 kg CO₂/GJ of energy, which is lower than that of anthracite coal (91.3 CO₂/GJ), gasoline (78.5 CO₂/GJ), and diesel (73.3 CO₂/GJ) [2]. Therefore, among the several areas of attention for further technological advances in the natural gas domain, storage, utilization, and supply chain are prominent in the downstream sector. The concept of natural gas storage is old and typically produced and, in some cases,

the processed gas is stored in an underground facility in the vicinity of the supply center. The stored gas is regularly monitored for potential loss and emission reliability of the supply chain to meet the customer demand is an important parameter for this form of energy [3]. The current issues related to the environment has led to adopting effective measures to handle major pollution sources and the transportation sector is considered as one of the important one among these. The use of natural gas owing to wide availability and its lower carbon emission compared to that of the higher hydrocarbons as fuel for vehicular application is projected to control the pollution level to a certain extent. Natural gas in two forms are utilized as vehicle fuel, i.e. compressed natural gas (CNG) and liquefied natural gas (LNG). The CNG is especially important for light vehicle transport such as cars and other cargo transporting vehicles, whereas the LNG form is utilized in industries and manufacturing along with domestic applications. However, these systems suffer from the limitations of high cost, low storage efficiency, and safety issues.

To improve the efficiency of the process, the concept of adsorbed natural gas (ANG) originated, in which the natural gas was stored in a comparatively high amount in a porous adsorbent system under ambient temperature conditions. In this process, the methane is believed to be adsorbed in molecular form in the nano-sized pores of the adsorbent network and the density in the adsorbed form exceeds the bulk density. The adsorption process being exothermic typically depended on the thermodynamic conditions. The amount of adsorption increased with a decrease in temperature and an increase in pressure. The ANG is considered to be a cost-effective alternative compared to that of liquefaction and energy-intensive compression. The storage pressure in this scenario can be decreased to ~35 bar compared to that of the utilized in CNG technology (200 bar) [4]. The target set by the Department of Energy (DOE) is $263 \text{ cm}^3/\text{cm}^3$ working capacity under standard conditions for the adsorbent material to be commercially viable. The value is gravimetrically equivalent to 0.5 g/g of adsorbent and amount of CNG at 200 bar and 25°C pressure and temperature respectively. Furthermore, the low energy density value of the natural gas also requires improvement which may be achieved by high-density packing so that it mimics the energy density value of LNG, i.e. ~22.2 MJ/L. Therefore, efficient adsorbents with high adsorption and desorption efficiency are desirable to utilize this ANG technology in an affordable manner for commercial implementation.

2. Materials for ANG storage

The selection of a suitable adsorbent is one of the most important criteria for the utilization of the technology for successful commercial application. An adsorbent with high surface area, large pore volume, narrow micropore distribution, the pore size of 1–1.2 nm, and high density is required to achieve the ambitious ANG storage target for vehicular application set by the US DOE. The porous materials studied in recent literature for adsorption based natural gas storage at relatively low pressure compared to that of the CNG and ambient temperature conditions are resins, zeolites [5], xerogels [6], aerogels, carbon-based materials [7] such as carbon nanotubes and fibers, metal organic frameworks (MOF) and covalent organic frameworks (COF). The methane adsorption efficiency is known to be linearly dependent on the surface area of the adsorbent (**Figure 1**) [8]. Earlier studies have revealed that Zeolites exhibiting adsorption capacity up to 100 V/V storage capacity are not suitable to reach the target set by the DOE and the interest has shifted to the carbon-based materials and 3D frameworks [4].

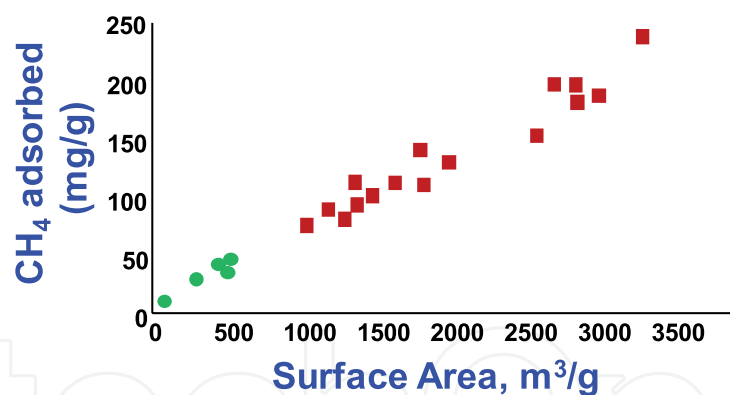


Figure 1. Schematics showing the effect of the surface of the carbon-based adsorbents on the methane uptake capacity, the red squares represent the carbon in granular powder form and the green circles represent the coal samples.

The volumetric storage capacity of the adsorbed natural gas may be calculated in a simple manner by following the equation given below;

$$n_{\text{stg}} = n_{\text{exc}} + \rho_{\text{gas}} \left[1 - \left(\rho_{\text{pack}} / \rho_{\text{He}} \right) \right] \quad (1)$$

where, n_{stg} is the volumetric storage capacity, n_{exc} is the excess amount of adsorbate per volume of adsorbent, ρ_{gas} , ρ_{pack} , and ρ_{He} is the gas, packing and helium density respectively.

2.1 Porous carbon materials

Porous carbon materials are one of the widely studied systems for said application. In general carbon-based materials have exhibited higher adsorption capacity compared to that of the other studied porous materials possessing similar surface area due to their slit-shaped pore structure [9]. The packing density of activated carbon-based materials is also known to exhibit a linear dependence on the applied pressure and the value reaches up to 0.8 g/cm³ on applying pressure till 980 MPa [10]. Furthermore, the activated carbon-based materials can be easily synthesized from readily available low-cost starting materials such as wooden materials, corns, different fossil fuels, and polymer and are cost-effective. These materials can be easily physically activated using steam or CO₂ and chemically activated in an industrial scale using acids and bases under high-temperature conditions [11]. Earlier studies on carbon-based adsorbent for the natural gas storage application was based on the single-walled carbon nanotubes (SWCNT). The Monte Carlo simulation-based theoretical studies predicted that the SWCNT bundles may be suitable for methane storage under moderate pressure conditions [12]. However, experimental studies afterward suggested that the adsorption capacity is limited to 0.11 g/g in these systems at 60 bar and 30°C [13]. The activated carbon-based materials have been successful in achieving excess gravimetric methane uptake till 0.2 g/g at 35 bar and ambient temperature conditions and in this case the delivery capacity was 170 V/V at 65 bar pressure [14]. Further increase in pressure to 100 bar improved the adsorption capacity to 263 V/V, which surpassed the target set by DOE. However, the deliverable capacity of carbon-based materials is reported to be inferior, which limits the utilization of these materials for storage applications. The carbon nanotube (CNT) though has shown promise to achieve high adsorption capacity, the experimental value is limited to 160 V/V at 35 bar and 25°C [15].

One of the advantages of these carbon-based materials is that these can be synthesized from renewable, polymeric, and cost-effective sources and activated via multiple routes. For example, olive stones were utilized to prepare carbon-based materials, which on carbonization at 500°C under inert atmosphere produced the carbon material. The sample was activated using KOH at a high temperature of 800°C [16]. The sample exhibited 3551 m²/g BET surface area and 215 V/V methane uptake capacity at 100 bar with a working capacity of 135 V/V. In another instance, polyacrylonitrile beads were pyrolyzed at 600°C to synthesize carbon flowers. The carbon flowers were then activated with KOH by heating the mixture at 800°C. The flowers were also activated by heating these under CO₂ flow at 850°C. The resulting carbon materials exhibited a BET surface area of 1077 m²/g and methane adsorption capacity of 196 V/V at 65 bar [17]. Other biomass precursors for the synthesis of porous carbon materials include coconut shells [18], corn straws [19], banana peels [20], and soya [21]. Xiao and coworkers published a summary on the use of various biomass for the synthesis of porous carbon materials and the surface area of the resulting materials [22]. The review also summarized the different activation methods utilized to activate the carbon materials such as strong inorganic bases [23], lewis acid [24], and H₃PO₄ [25] based procedures to optimize the pore structure further and enhance their adsorption performance. Templating is another useful technique utilized in literature to achieve highly ordered and large surface area carbon materials. Both soft and hard templating can be used for this purpose. Hard templates could be a various nanoparticles, silica, and molecular sieves. For example, mesoporous silica sieve hard templates in presence of 1,10-phenanthroline ligand were utilized to synthesize Co immobilized nitrogen-doped porous carbon materials for catalytic applications. The calcination for the material synthesis was carried out at 800°C [26]. Typically, in the case of the soft templating method, the polymers or surfactant self-assemble into a particular ordered shape, which is then immobilized into the mesoporous material to be synthesized. Subsequently, the templates are removed to expose the pores and obtain the porous material. Ionic liquid and self-assembled block polymers have been utilized as the soft templates for this purpose [27, 28]. Direct carbonization of ordered nanostructures is also becoming another attractive option to generate porous carbon materials. For example, the MOF can be utilized as precursors to directly synthesize porous carbon materials via pyrolysis under an inert environment [29]. The presence of various organic ligands may also serve as the carbon source for the above synthesis, whereas the metal nodes often help to control the pore structure and control the physical properties of the carbon material. For example, Yamaguchi and coworkers utilized a Zn and Co-based bimetallic MOF to synthesize nanoporous carbon by pyrolyzing the precursor under an inert atmosphere at 900°C [30]. The shape of the precursor was replicated in the carbon material produced as can be shown in **Figure 2** below. Metal such as Zn evaporates at a high temperature allowing the formation of pores in the resulting carbon product. In some cases, the metal ions convert to the corresponding nanoparticles and serve as a catalytic site for further applications. The type of metal, the metal content, and ligand type play important role in developing nanoporous carbon structures.

2.2 Metal organic frameworks

In this regard, the MOFs have gained strong interest in their ability to reversibly store natural gas for vehicular application. MOFs are a wide family of reticular and highly porous coordination polymers formed by the coordination self-assembly of the metal center with multidentate organic building blocks [32, 33]. The MOFs are reported to exhibit ultra-high surface area up to 10,000 m²/g, and tunable pore sizes

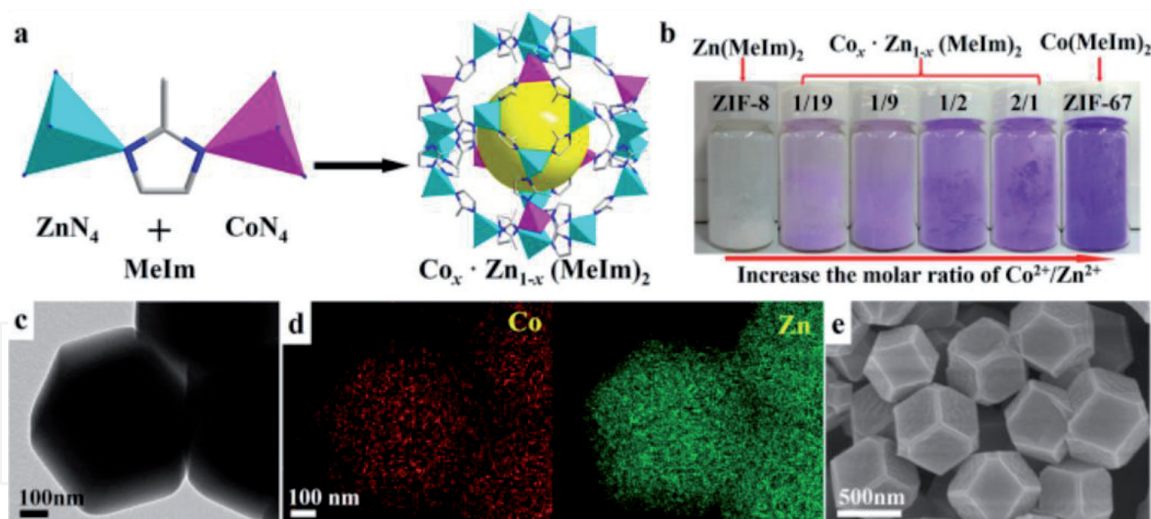


Figure 2. (a) The crystal structure of Zn and Co-based bimetallic MOF, (b) the photographs of solutions possessing different molar ratios of Co^{2+} to Zn^{2+} , (c and d) the TEM and (e) SEM images of the MOF and produced nanoporous carbon., Reproduced with permission from [30]. Copyright 2016 Nature Publishing Group. The elemental mapping images show the presence of Co and Zn in the parent system.

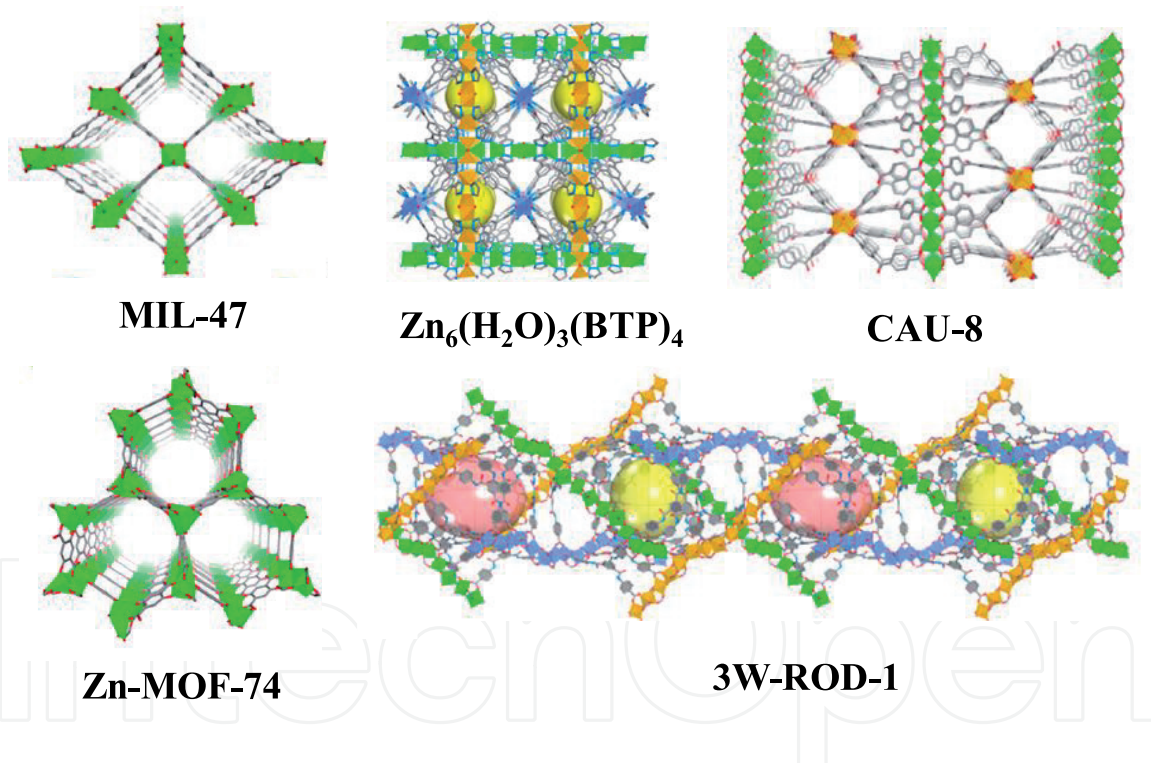


Figure 3. Structure of some of the rod MOFs synthesized in recent literature. Reproduced with permission from [31], Copyright 2021, American Chemical Society.

with the possibility to functionalize them [34]. A number of MOF materials such as MIL-74, CAU-8, $\text{Zn}_6(\text{H}_2\text{O})_3(\text{BTP})_4$, Zn-MOF-74, 3W-ROD-1, and Ni-MOF-74 are studied towards their ability to store natural gas (**Figure 3**) [31]. Similarly, Pore size optimization is one of the important targets in the field of MOF materials. The effective way to address the same is by gradually changing the length of the organic linker and introducing functionality into the linker. For example, the introduction of sulfone and carbonyl groups notably improved the CO_2 absorption capacity compared to that of the un-functionalized one (**Figure 4**) [35].

For an adsorbent to exhibit adequate adsorption ability, the system should maintain a balance between gravimetric (SA_G) and volumetric surface area (SA_V)

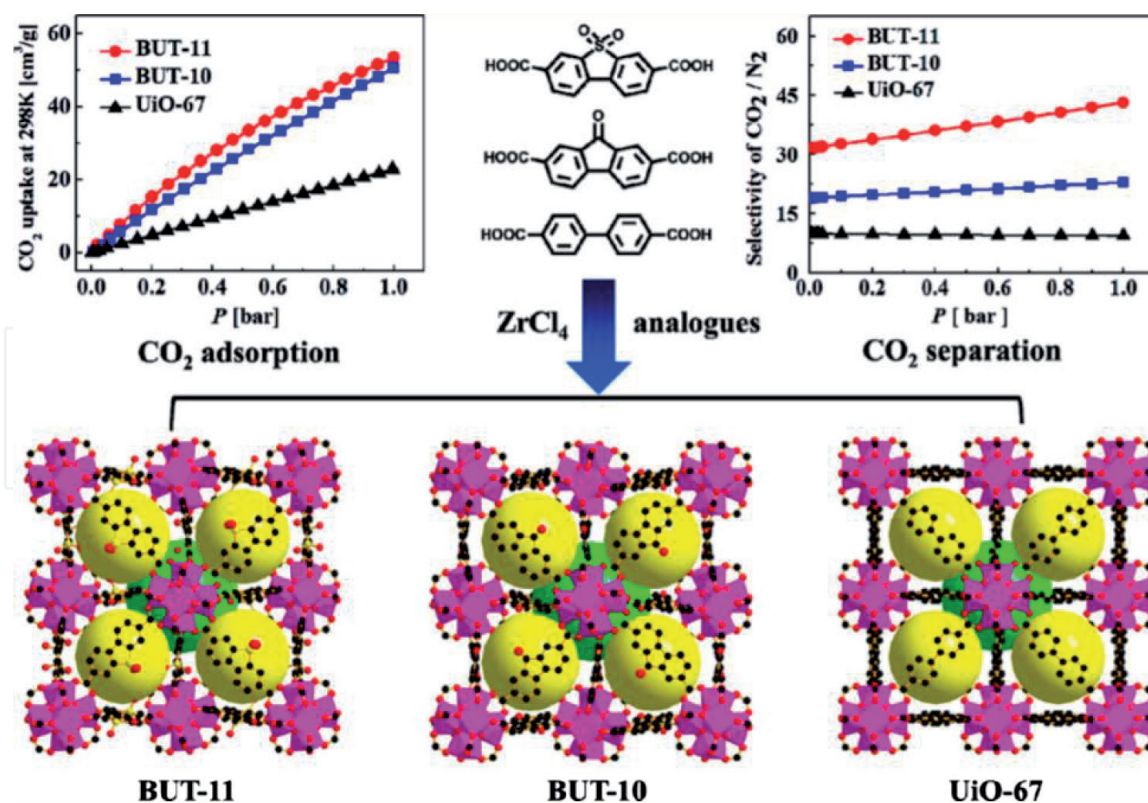


Figure 4. Effect of ligand size on the pore structure of the resulting MOFs. Reproduced with permission from [35], Copyright 2014, American Chemical Society.

along with high porosity. Often the normalized value of the product of SA_G and SA_V is utilized to suggest the above. It is known that the helium void fraction displays a volcano relationship with the largest pore diameter. The NU-1500; Al and PET-based MOF systems exhibit void fraction and largest pore diameter values of 0.76 and 12.7 Å respectively and display high CH₄ storage capacity. A similar system with Fe at the coordinating center, the NU-1501 series displayed increased VF values of 0.87 and an LPD value of 18.8 Å [36]. The MOF series based on extended PET system and Al metal displayed SA_G and SA_V of 7310 m²/g and 2060 m²/cm³ respectively. The corresponding Fe-based system showed a somewhat lower SA_G value (7140 m²/g) and comparable SA_V value (2130 m²/cm³). The study showed that the SA_G and SA_V values can be controlled further to significantly improve the gravimetric uptake capacity while retaining the volumetric storage capacity.

The gas adsorption capacity and separation performance of the MOFs may be optimized further by suitably modifying the organic building blocks with functional groups using simple organic transformation. The presence of polar functional groups in the mainframe of MOFs effectively improves the CO₂ capture and separation abilities. For example, MOF is based on flexible hexadentate ligands containing amide groups, N-tris-isophthalic acid-1,3,5-benzenetricarboxamide (TPBTM) such as [Cu₂₄(TPBTM⁶⁻)₈(H₂O)₂₄] (Cu-TPBTM) with high surface area [37]. The pore structure of the resulting MOFs depended on the size, structure, and functionality of the organic building blocks as shown in **Figure 5** for representative purposes.

These class of materials are reported to exhibit adsorption capacity up to 180 V/V. For example, the HKUST-1 based on Cu metal and 1,3,5-benzenetricarboxylate organic linker exhibits surface area up to 1800 m²/g with adequate stability [37]. Similarly, a MOF system based on Cu and a hexadentate linker 3,3',3'',5,5',5''-benzene-1,3,5-triyl-hexabenzic acid exhibited BET surface area up to 6240 m²/g [39]. The open metal site in these MOFs serves as the site to bind to the methane molecule. At 100 bar pressure and 25°C, these MOFs display

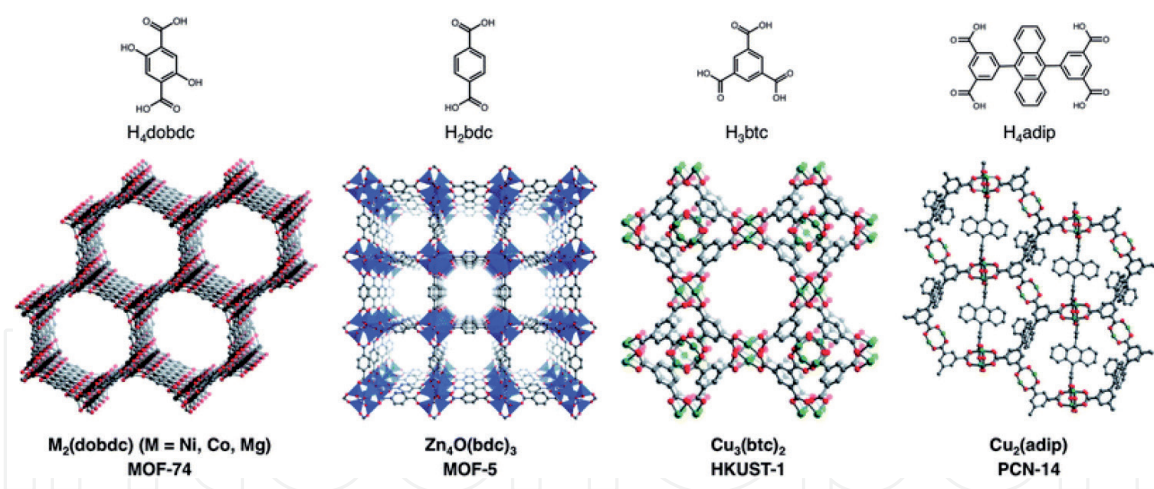


Figure 5.
 The Cu-TPNTM MOFs and their pore structure is depicted above. Reproduced with permission from [38].
 Copyright 2014, Royal Society of Chemistry.

storage capacity up to 330 V/V. The issue with this MOF system towards practical applications is that higher hydrocarbons, such as ethane and propane adsorb more strongly compared to that of the methane and tend to block the pore site [40]. Seki reported a MOF system, based on copper and triethylenediamine (TED), $[\text{Cu}-(\text{O}_2\text{CRCO}_2) \cdot 1/2\text{TED}]_n$ $[\text{R} = 4,4'\text{-C}_6\text{H}_4\text{C}_6\text{H}_4 \text{ (1)}]$ which recorded a volumetric storage capacity for methane up to 225 V/V [41]. For the synthesis of MOFs for said application, key factors such as the number of coordinating sites, size, shape, and geometric configuration of organic linkers require careful attention, which determines the self-assembled structure and gas adsorption performance of MOFs. Typically, the coordinating sites of the organic building blocks consist of electron-donating elements such as O, S, and N. Among the corresponding coordinating functionalities, the carboxylic acid groups tend to form stable MOFs. A set of crystalline MOFs based on 4,4',4''-[benzene-1,3,5-triyl-tris(ethyne-2,1-diyl)] tribenzoate organic linker and $\text{Zn}_4\text{O}(\text{CO}_2)_6$ was synthesized that exhibited non-interpenetrating 3D crystal structures with pores of $\sim 48 \text{ \AA}$ sizes [42]. The MOF displayed an extremely high BET surface area of $6240 \text{ m}^2/\text{g}$. A table summarizing the adsorption capacity under given temperature and pressure conditions for various MOFs is included for reference (**Table 1**) [43].

Considering the gas density in the pores of the adsorbent to be considerably higher compared to that of the bulk density, the optimization of void space becomes important to maximize the adsorption capacity. Therefore, monoliths of MOFs are prepared using compression, binder, and polymeric additives [45]. However, the use of additives though known to improve the mechanical strength has their drawback as these tend to block the pore space and decrease the uptake capacity [46]. Therefore, preparation of pure monolith of MOF using compression has been pursued in literature. Even mechanical compression notably decreased the uptake capacity possibly due to the collapse of the pore structure. For example, the uptake capacity of $\text{Ni}_2(1,4\text{-dioxido-2,5-benzenedicarboxylate})$ based MOF decreased from 230 to 100 V/V at 34 bar and 30°C after palletization [47]. Another way to handle the issue is to use a sol-gel technology in which gradual evaporation of solvent from the monoliths without destroying the pore structure. Recently, HKUST-1 monolith prepared using sol-gel technique exhibited uptake capacity of 259 V/V at 65 bar and 25°C [48].

The methane binding sites were studied in the literature on Zn-based MOF samples using low-temperature synchrotron analysis. The data revealed two primary adsorption sites and one secondary adsorption site. The primary adsorption sites

MOFs	BET	Pressure	Capacity (cm ³ /g)	Reference
	(m ² /g)	(bar)		
NU-1500-Al	3650	100	549.1	[43]
MOF-177	4500	65	475	[38]
NU-1501-Al	7310	100	929.7	[43]
PCN-46	2500	65	310.7	[43]
PCN-61	3000	65	366.8	[43]
PCN-66	4000	65	397.9	[43]
PCN-68	5109	65	465.2	[43]
UTSA-61	2171	65	337	[43]
UTSA-20	1620	65	252.7	[43]
NOTT-119	4118	65	426.6	[43]
NU-111	4930	65	503	[43]
NU-125	3286	65	395	[43]
NU-140	4300	65	451.5	[43]
NOTT-100	1661	35	210	[43]
NOTT-102	3342	35	308	[38]
UTSA-110	3241	65	402	[44]
UTSA-76	2820	65	363	[44]
NJU-Bai-43	3090	65	396	[44]
LIFM-82	1624	65	267	[44]
MFM-38	2022	65	346	[44]
MFM-115a	3394	65	389	[44]
MIL-53 (Cr)	1500 (Langmuir)	35	159	[38]
SNU-77	3670	35	250	[38]
PCN-68	5109	35	332	[38]
IRMOF	1102	35	163	[38]
DUT-4	1308	35	158	[38]
FJI-1	4043	35	273	[38]
DUT-13	5570 (Langmuir)	35	250	[38]
MOF-210	6240	35	331	[38]
DUT-8 (Co)	1400	35	78	[38]

Table 1.
The methane gas adsorption capacity of various MOFs under different pressures conditions [38, 43, 44].

were located near the Zn complex paddlewheel and the center of the small windows was recognized as the second primary adsorption site. At these sites, the methane interacted with the phenyl units and paddlewheel units. The secondary adsorption site was recognized as the center of the cavity [49]. However, still, the interaction of functional groups with methane is not very clear. More studies with support from spectroscopic tools may be necessary for future to completely ascertain the mechanism of methane storage. Using flexible MOFs is attractive to improve desorption capacity and minimize the loss during desorption. Considering the desorption pressure of the working engine is fixed at 4.8 bar by DoE, the reported flexible

MOFs are known to absorb ANG at between 35 and 65 bar and release most of the gas at ~5 bar pressure [50, 51]. The type of metal center in the MOF also controls the uptake capacity and thermal management of the system. For example, Co(bdp) and Fe(bdp) based MOFs through exhibit comparable methane uptake capacity, Fe-based system has desorption steps at higher pressures of 10 bar compared to that of the Co-based system [52]. Similarly, in terms of intrinsic thermal management, the amount of heat released by Fe(bdp) based system (64.3 kJ/L) is 12% compared to that of the Co(bdp) (73.4 kJ/L) based system. Overall, the challenge with these systems lies with the fact that the 3D structure to be produced in such a way that the aromatic rings are exposed for the CH₄ interaction. However, expansion of the organic linkers leads to fragile materials and allows for the self-interpenetration of lattices. Furthermore, the thermal stability of the coordination linkage, low heat of adsorption, and high packing density are also important from the perspective of commercial viability. Keeping in view of the above, suitable MOFs with high surface area and porosity may be designed and synthesized for the ANG storage application.

2.3 Covalent organic frameworks

Another exciting avenue for reversible storage of CH₄ is the covalent organic frameworks (COFs). The COFs are nanoporous materials formed by the covalent crosslinking of organic functional groups. These are lightweight materials with large pore volume, low density, and presence of hydrocarbon frames that enhances the interaction towards CH₄ and improve the uptake capacity. Importantly, these possess high thermal stability and low molecular weight. For example, the COFs based on boronic acid linkage exhibited high thermal stability till 500°C and surface area up to 1590 cm²/g [53]. The surface area of boronic acid-based COFs increased further by restructuring the pore structure through the incorporation of two nodes, i.e. triangular (ctn) and tetrahedral (bor). The surface area of the COFs was measured to be 4210 cm²/g [54]. Earlier studies have proposed to minimize the methane COF interaction and increase the heat of adsorption to enhance the delivery efficiency of methane. These studies have further proposed that substitution on the phenyl ring does not alter the binding ability in the samples [55].

A study based on aromatic imine networks revealed that sub-stoichiometric construction of COFs hexagonal building blocks with four connecting sites, where the two unreacted sites can be used to enhance the selectivity of hydrocarbon adsorption [56]. The COF displayed a high BET surface area up to 3478 m²/g and methane adsorption capacity of 11.2 cm³/g. Similarly, another sub-stoichiometric COFs based on imines displaying bex net topology synthesized using tri- and tetratopic linkers are reported in the literature [57]. Topology control in COF is another important aspect to control the uptake capacity. For example, recently an N,N-dimethyl acetamide and 1,3,5-trimethylbenzene based imine-COF was synthesized that displayed two different types of triangular micropores of different pore dimensions. The diameter of the pores was 11.3 and 15.2 Å respectively [58]. The COFs with tbo topology have been reported in the literature by using planar porphyrin with four coordinating sites and 3 coordinating trigonal aldehydes of a triphenylamine. The COFs are arranged into a $Pm\bar{3}$ space group and constitute a non-interpenetrating framework [59].

COFs possessing pcu topology have been synthesized using distorted aromatic compounds serving as triangular antiprismatic nodes [60]. Imine-based COFs possessing fjh topology was synthesized by coupling a triangular linker with a square building block [61]. Triptycene-based COFs displaying a non-interpenetrated ceq or acs topology was synthesized using a combination of a triangular prism and

planar triangle nodes [44]. The sample displayed methane adsorption capacity up to $48 \text{ cm}^3/\text{g}$ at 0°C and 1 bar. The COF exhibited a BET surface area value of $2650 \text{ m}^2/\text{g}$. Overall, studies have shown that the organic building block structure and functionality can be utilized as a control to develop COFs with controlled pore size, pore structure, and topology. The functionality in the COF system may be introduced to enhance the selectivity of such systems towards methane adsorption compared to that of the polar gases. The stoichiometry also serves as one of the handles to control the topology of the COFs. Several studies have shown that these materials possessing adequate thermal stability and binding ability towards methane may be a useful option for methane storage applications.

3. Conclusion


To summarize, ANG holds strong promise in the area of fuel for transportation and other consumer sectors. The affordability depends on the availability of cost-effective adsorbents with high storage capacity with optimized deliverability. Though porous carbon, metal-organic framework, and covalent organic framework have shown promise, the target set by the DOE is yet to be complied with optimum deliverability. Selective compositions have been successful in achieving the storage capacity limits, the cost-effective and large scale production of such materials is under ways to materialize a commercializable product. These porous nanostructures are predicted to reach a high surface area up to $4000 \text{ m}^2/\text{g}$ and beyond. A greater understanding of the pore structure, synthetic process, and mechanism of formation, pore controlling factors during synthesis and factors contributing towards the pore uniformity and stability would notably help towards the development of nonporous materials with high surface area and controlled pore structure. Therefore, the development of new cost-effective, thermally stable adsorbents with high uptake capacity and material strength is still desirable to further fulfill the commercial viability aspect of the technology.

Author details

Akhoury Sudhir Kumar Sinha*, Umaprasana Ojha,
Marriyappan Sivagnanam Balathanigaimani and Sanjay Kar
Rajiv Gandhi Institute of Petroleum Technology, Jais, Uttar Pradesh, India

*Address all correspondence to: asksinha@rgipt.ac.in

IntechOpen

© 2021 The Author(s). Licensee IntechOpen. This chapter is distributed under the terms of the Creative Commons Attribution License (<http://creativecommons.org/licenses/by/3.0>), which permits unrestricted use, distribution, and reproduction in any medium, provided the original work is properly cited. 

References

- [1] Saha D, Grappe HA, Chakraborty A, Orkoulas G. Postextraction separation, on-board storage, and catalytic conversion of methane in natural gas: A review. *Chemical Reviews*. 2016;**116**(19):11436-11499
- [2] Sapag K, Vallone A, Garca A, Solar C. Adsorption of methane in porous materials as the basis for the storage of natural gas. In: *Natural Gas*. IntechOpen; 2010. DOI: 10.5772/9846
- [3] Alden CB, Wright RJ, Coburn SC, Caputi D, Wendland G, Rybchuk A, et al. Temporal variability of emissions revealed by continuous, long-term monitoring of an underground natural gas storage facility. *Environmental Science and Technology*. 2020;**54**(22):14589-14597
- [4] Wegrzyn J, Gurevich M. Adsorbent storage of natural gas. *Applied Energy*. 1996;**55**:71-83
- [5] Zhang SY, Talu O, Hayhurst DT. High-pressure adsorption of methane in zeolites NaX, MgX, CaX, SrX and BaX. *The Journal of Physical Chemistry*. 1991;**95**:1722-1726
- [6] MacGibbon R, Badheka R, Sermon P. Organically-modified silica xerogels for adsorption of CH₄ at 298 K. *Journal of Sol-Gel Science and Technology*. 2004;**32**:53-56
- [7] Rodríguez-Reinoso F, Almansa C, Molina-Sabio M. Contribution to the evaluation of density of methane adsorbed on activated carbon. *Journal of Physical Chemistry B*. 2005;**109**(43): 20227-20231
- [8] Menon VC, Komarneni S. Porous adsorbents for vehicular natural gas storage: A review. *Journal of Porous Materials*. 1998;**5**:43-58
- [9] Pfeifer P, Ehrburger-Dolle F, Rieker T, González M, Hoffman W, Molina-Sabio M, et al. Nearly space-filling fractal networks of carbon nanopores. *Physical Review Letters*. 2002;**88**:115502
- [10] Im JS, Jung MJ, Lee YS. Effects of fluorination modification on pore size controlled electrospun activated carbon fibers for high capacity methane storage. *Journal of Colloid and Interface Science*. 2009;**339**(1):31-35
- [11] Tsivadze AY, Aksyutin OE, Ishkov AG, Men'shchikov IE, Fomkin AA, Shkolin AV, et al. Porous carbon-based adsorption systems for natural gas (methane) storage. *Russian Chemical Reviews*. 2018;**87**(10):950-983
- [12] Kowalczyk P, Solarz L, Do DD, Samborski A, MacElroy JMD. Nanoscale tubular vessels for storage of methane at ambient temperatures. *Langmuir*. 2006;**22**(21):9035-9040
- [13] Yang CM, Noguchi H, Murata K, Yudasaka M, Hashimoto A, Iijima S, et al. Highly ultramicroporous single-walled carbon nanohorn assemblies. *Advanced Materials*. 2005;**17**(7):866-870
- [14] Kaneko K, Rodríguez-Reinoso F. *Nanoporous Materials for Gas Storage*. Berlin, Germany: Springer; 2019
- [15] Kumar KV, Preuss K, Titirici MM, Rodríguez-Reinoso F. Nanoporous materials for the onboard storage of natural gas. *Chemical Reviews*. 2017;**117**(3):1796-1825
- [16] Casco ME, Martínez-Escandell M, Gadea-Ramos E, Kaneko K, Silvestre-Albero J, Rodríguez-Reinoso F. High-pressure methane storage in porous materials: Are carbon materials in the pole position? *Chemistry of Materials*. 2015;**27**(3):959-964

- [17] Chen S, Gong H, Dindoruk B, He J, Bao Z. Dense carbon nanoflower pellets for methane storage. *ACS Applied Nano Materials*. 2020;**3**(8):8278-8285
- [18] Yue L, Xia Q, Wang L, Wang L, DaCosta H, Yang J, et al. CO₂ adsorption at nitrogen-doped carbons prepared by K₂CO₃ activation of urea-modified coconut shell. *Journal of Colloid and Interface Science*. 2018;**511**:259-267
- [19] Qiu Z, Wang Y, Bi X, Zhou T, Zhou J, Zhao J, et al. Biochar-based carbons with hierarchical micro-meso-macro porosity for high rate and long cycle life supercapacitors. *Journal of Power Sources*. 2018;**376**:82-90
- [20] Fasakin O, Dangbegnon JK, Momodu DY, Madito MJ, Oyedotun KO, Eleruja MA, et al. Synthesis and characterization of porous carbon derived from activated banana peels with hierarchical porosity for improved electrochemical performance. *Electrochimica Acta*. 2018;**262**:187-196
- [21] Rana M, Subramani K, Sathish M, Gautam UK. Soya derived heteroatom doped carbon as a promising platform for oxygen reduction, supercapacitor and CO₂ capture. *Carbon*. 2017;**114**:679-689
- [22] Li B, Xiong H, Xiao Y. Progress on synthesis and applications of porous carbon materials. *International Journal of Electrochemical Science*. 2020;**15**(2):1363-1377
- [23] Liang C, Bao J, Li C, Huang H, Chen C, Lou Y, et al. One-dimensional hierarchically porous carbon from biomass with high capacitance as supercapacitor materials. *Microporous and Mesoporous Materials*. 2017;**251**:77-82
- [24] Wu Z, Wee V, Ma X, Zhao D. Adsorbed natural gas storage for onboard applications. *Advanced Sustainable Systems*. 2021;**5**(4):1-16
- [25] Yorgun S, Yildiz D. Preparation and characterization of activated carbons from Paulownia wood by chemical activation with H₃PO₄. *Journal of the Taiwan Institute of Chemical Engineers*. 2015;**53**:122-131
- [26] Zhang L, Wang J, Shang N, Gao S, Gao Y, Wang C. Ultra dispersed cobalt anchored on nitrogen-doping ordered porous carbon as an efficient transfer hydrogenation catalyst. *Applied Surface Science*. 2019;**491**:544-552
- [27] Du J, Liu L, Yu Y, Zhang Y, Chen A. N-doping carbon sheet and core-shell mesoporous carbon sphere composite for high-performance supercapacitor. *Journal of Industrial and Engineering Chemistry*. 2019;**76**:450-456
- [28] Libbrecht W, Verberckmoes A, Thybaut JW, Van Der Voort P, De Clercq J. Tunable large pore mesoporous carbons for the enhanced adsorption of humic acid. *Langmuir*. 2017;**33**(27):6769-6777
- [29] Chu X, Meng F, Deng T, Zhang W. Metal organic framework derived porous carbon materials excel as an excellent platform for high-performance packaged supercapacitors. *Nanoscale*. 2021;**13**(11):5570-5593
- [30] Tang J, Salunkhe RR, Zhang H, Malgras V, Ahamad T, Alshehri SM, et al. Bimetallic metal-organic frameworks for controlled catalytic graphitization of nanoporous carbons. *Scientific Reports*. 2016;**6**:3-4
- [31] Zhang Y-F, Zhang Z-H, Ritter L, Fang H, Wang Q, Space B, et al. New reticular chemistry of the rod secondary building unit: Synthesis, structure, and natural gas storage of a series of three-way rod amide-functionalized metal-organic frameworks. *Journal of the American Chemical Society*. 2021;**143**:12202-12211
- [32] Yan Y, Kolokolov DI, Da Silva I, Stepanov AG, Blake AJ, Dailly A, et al.

Porous metal-organic polyhedral frameworks with optimal molecular dynamics and pore geometry for methane storage. *Journal of the American Chemical Society*. 2017;**139**(38):13349-13360

[33] Kirchon A, Feng L, Drake HF, Joseph EA, Zhou HC. From fundamentals to applications: A toolbox for robust and multifunctional MOF materials. *Chemical Society Reviews*. 2018;**47**(23):8611-8638

[34] Choi PS, Jeong JM, Choi YK, Kim MS, Shin GJ, Park SJ. A review: Methane capture by nanoporous carbon materials for automobiles. *Carbon Letters*. 2016;**17**(1):18-28

[35] Wang B, Huang H, Lv XL, Xie Y, Li M, Li JR. Tuning CO₂ selective adsorption over N₂ and CH₄ in UiO-67 analogues through ligand functionalization. *Inorganic Chemistry*. 2014;**53**(17):9254-9259

[36] Chen Z, Li P, Anderson R, Wang X, Zhang X, Robison L, et al. Balancing volumetric and gravimetric uptake in highly porous materials for clean energy. *Science*. 2020;**368**(6488):297-303

[37] Zheng B, Bai J, Duan J, Wojtas L, Zaworotko MJ. Enhanced CO₂ binding affinity of a high-uptake rht-type. *Journal of the American Chemical Society*. 2011;**133**:748-751

[38] Mason JA, Veenstra M, Long JR. Evaluating metal-organic framework for natural gas storage. *Chemical Science*. 2014;**5**:32-35

[39] Guo Z, Wu H, Srinivas G, Zhou Y, Xiang S, Chen Z, et al. A metal-organic framework with optimized open metal sites and pore spaces for high methane storage at room temperature. *Angewandte Chemie. International Edition*. 2011;**50**(14):3178-3181

[40] Hang H, Deria P, Farha OK, Hupp JT, Snurr RQ. A thermodynamic

tank model for studying the effect of higher hydrocarbons on natural gas storage in metal-organic frameworks. *Energy and Environmental Science*. 2015;**8**(5):1501-1510

[41] Seki K. Design of an adsorbent with an ideal pore structure for methane adsorption using metal complexes. *Chemical Communications*. 2001;**1**(16):1496-1497

[42] Furukawa H, Ko N, Go YB, Aratani N, Choi SB, Choi E, et al. Ultrahigh porosity in metal-organic frameworks. *Science*. 2010;**329**(5990):424-428

[43] Fan W, Zhang X, Kang Z, Liu X, Sun D. Isoreticular chemistry within metal-organic frameworks for gas storage and separation. *Coordination Chemistry Reviews*. 2021;**443**:213968

[44] Li H, Chen F, Guan X, Li J, Li C, Tang B, et al. Three-dimensional triptycene-based covalent organic frameworks with ceq or acs topology. *Journal of the American Chemical Society*. 2021;**143**(7):2654-2659

[45] Rubio-Martinez M, Avci-Camur C, Thornton AW, Imaz I, Maspocho D, Hill MR. New synthetic routes towards MOF production at scale. *Chemical Society Reviews*. 2017;**46**(11):3453-3480

[46] Zhu H, Yang X, Cranston ED, Zhu S. Flexible and porous nanocellulose aerogels with high loadings of metal-organic-framework particles for separations applications. *Advanced Materials*. 2016;**28**(35):7652-7657

[47] Tagliabue M, Rizzo C, Millini R, Dietzel PDC, Blom R, Zanardi S. Methane storage on CPO-27-Ni pellets. *Journal of Porous Materials*. 2011;**18**(3):289-296

[48] Bueken B, Van Velthoven N, Willhammar T, Stassin T, Stassen I,

- Keen DA, et al. Gel-based morphological design of zirconium metal-organic frameworks. *Chemical Science*. 2017;**8**(5):3939-3948
- [49] Kim H, Samsonenko DG, Das S, Kim GH, Lee HS, Dybtsev DN, et al. Methane sorption and structural characterization of the sorption sites in $\text{Zn}_2(\text{bdc})_2(\text{dabco})$ by single crystal x-ray crystallography. *Chemistry—An Asian Journal*. 2009;**4**(6):886-891
- [50] Li H, Wang K, Sun Y, Lollar CT, Li J, Zhou HC. Recent advances in gas storage and separation using metal-organic frameworks. *Materials Today*. 2018;**21**(2):108-121
- [51] Bolinois L, Kundu T, Wang X, Wang Y, Hu Z, Koh K, et al. Breathing-induced new phase transition in an $\text{MIL-53}(\text{Al})-\text{NH}_2$ metal-organic framework under high methane pressures. *Chemical Communications*. 2017;**53**(58):8118-8121
- [52] He Y, Chen F, Li B, Qian G, Zhou W, Chen B. Porous metal-organic frameworks for fuel storage. *Coordination Chemistry Reviews*. 2018;**373**:167-198
- [53] Côté AP, Benin AI, Ockwig NW, O’Keeffe M, Matzger AJ, Yaghi OM. Chemistry: Porous, crystalline, covalent organic frameworks. *Science*. 2005;**310**(5751):1166-1170
- [54] El-Kaderi HM, Hunt JR, Mendoza-Cortés JL, Côté AP, Taylor RE, O’Keeffe M, et al. Designed synthesis of 3D covalent organic frameworks. *Science*. 2007;**316**(5822):268-272
- [55] Mendoza-Cortes JL, Pascal TA, Goddard WA. Design of covalent organic frameworks for methane storage. *Journal of Physical Chemistry A*. 2011;**115**(47):13852-13857
- [56] Chen L, Gong C, Wang X, Dai F, Huang M, Wu X, et al. Substoichiometric 3D covalent organic frameworks based on hexagonal linkers. *Journal of the American Chemical Society*. 2021;**143**(27):10243-10249
- [57] Banerjee T, Haase F, Trenker S, Biswal BP, Savasci G, Duppel V, et al. Sub-stoichiometric 2D covalent organic frameworks from tri- and tetratopic linkers. *Nature Communications*. 2019;**10**(1):1-10
- [58] Xu SQ, Zhan TG, Wen Q, Pang ZF, Zhao X. Diversity of covalent organic frameworks (COFs): A 2D COF containing two kinds of triangular micropores of different sizes. *ACS Macro Letters*. 2016;**5**(1):99-102
- [59] Kang X, Han X, Yuan C, Cheng C, Liu Y, Cui Y. Reticular synthesis of tbo topology covalent organic frameworks. *Journal of the American Chemical Society*. 2020;**142**(38):16346-16356
- [60] Martínez-Abadía M, Strutyński K, Lerma-Berlanga B, Stoppiello CT, Khlobystov AN, Martí-Gastaldo C, et al. π -Interpenetrated 3D covalent organic frameworks from distorted polycyclic aromatic hydrocarbons. *Angewandte Chemie*. 2021;**133**(18):10029-10034
- [61] Nguyen HL, Gropp C, Ma Y, Zhu C, Yaghi OM. 3D covalent organic frameworks selectively crystallized through conformational design. *Journal of the American Chemical Society*. 2020;**142**(48):20335-20339